

Modification of spectral UV irradiance by clouds

Harry Schwander and Peter Koepke

Meteorologisches Institut der Universität München, Munich, Germany

Anton Kaifel

Zentrum für Sonnenenergie- und Wasserstoff-Forschung, Stuttgart, Germany

Gunther Seckmeyer

Institut für Meteorologie und Klimatologie, Hannover, Germany

Received 17 September 2001; revised 14 December 2001; accepted 17 December 2001; published 27 August 2002.

[1] Approximately 10,000 UV irradiance spectra resulting from 2 years of continuous measurements in Germany were used as a database to analyze the effect of cloudiness on spectral UV irradiance. Values of spectral cloud modification factors (CMF) were derived by modeling a corresponding clear-sky irradiance spectrum for every UV measurement under cloudy conditions. The total set of CMF values was used to train neural networks using different sets of input data (parameter records) to describe the clouds, resulting in different, optimized, algorithms (CMF parameterizations). These different CMF parameterizations were evaluated by asking how the quality of the derived CMFs depended on the information content of different parameter records. It was shown that a visual description of cloudiness is not adequate to determine CMFs for an actual case (deviations of 50% and more), even if it was known whether or not the solar disk was obscured by clouds. Improvements for the determination of actual CMFs are possible, with deviations mostly below 15% if the parameter record comprises an actual broadband irradiance measurement. It was shown that such a CMF parameterization is able to provide a good estimation of actual CMFs, also for places with a different cloud climatology. The sensitivity of CMFs to wavelength and solar zenith angle was investigated on the basis of the derived CMF parameterizations. The relations found depend on the kind of CMF parameterization, i.e., the parameter record. In particular the separation of those cases when the solar disk is visible from those cases when the solar disk is obscured may lead to different dependencies of CMFs on solar zenith angle and wavelength.

INDEX TERMS:

0360 Atmospheric Composition and Structure: Transmission and scattering of radiation; 3337 Meteorology and Atmospheric Dynamics: Numerical modeling and data assimilation; 3359 Meteorology and Atmospheric Dynamics: Radiative processes; 3367 Meteorology and Atmospheric Dynamics: Theoretical modeling;

KEYWORDS: clouds, cloud modification factor, neural networks, UV radiation, UV measurement, UV modeling

1. Introduction

[2] The detection of the Antarctic ozone hole [Stolarski *et al.*, 1991; Gleason *et al.*, 1993] and the significant increase in skin cancer in several regions of the world, that is, at least partly, supposed to be UV induced [Cascinelli and Marchesini, 1989; Koh *et al.*, 1990], has led to strong research activities in the field of UV radiation in recent years. These activities yield both a worldwide monitoring of UV radiation levels [e.g., Seckmeyer *et al.*, 1995] and a deep understanding of the atmospheric processes that influence UV radiation [Schwander *et al.*, 1997; Weihs and Webb, 1997; Forster, 1995]. Clouds are, together with solar zenith angle and total ozone amount, the most important factor influencing ground level UV radiation [e.g., Burrows, 1997]. The

numerical description of clouds radiative influence yields special complications. The main reason is the large variability of clouds, which often occur as horizontally inhomogeneous cloud fields. Thus, information to describe the radiative properties of actual cloud conditions is generally poor. Moreover, the commonly used one-dimensional models are not able to deal with scattered clouds.

[3] A common approach to model global irradiance for skies with broken cloudiness is the combination of the result of a clear-sky model with a factor to describe the cloud influence, in the following called cloud modification factor, CMF:

$$CMF = E_{\text{cloud}}/E_{\text{clear}}, \quad (1)$$

where E_{cloud} is the global irradiance in the presence of clouds and E_{clear} is the global irradiance for the same atmospheric conditions but for a cloudless atmosphere. All

quantities in equation (1) might be considered spectrally dependent.

[4] Here the basic aspects with respect to CMFs will be first discussed together with the nomenclature that will be used in the following. From a UV irradiance value under cloudy conditions in combination with an irradiance value for the corresponding clear-sky conditions, an individual CMF value can be determined. The irradiance for the cloudy condition is always determined by measurement, while the clear-sky irradiance either is taken from measurements or is modeled. The latter is given preference since appropriate corresponding values (at least in solar zenith angle, ozone amount, aerosol properties and surface albedo) are often not available. To model UV irradiance under cloudy conditions with a one-dimensional model, using of equation (1), a CMF that is derived from the available information for the actual cloudiness must be available. To get such data, a CMF parameterization is necessary. Such a parameterization is determined by the correlation of many measured CMF values with an appropriate description of the corresponding cloud properties. The methods to describe the cloud properties (the parameter records) may be different, resulting in different CMF parameterizations. The simplest method is the total cloud amount; more detailed would be the cloud amount for different cloud types or cloud heights, or additionally the information whether the Sun is obscured by a cloud or not. In any case, the application of such a CMF parameterization results in CMFs that are average values with respect to the given cloud situation.

[5] Different CMF parameterizations can be found in the literature [e.g., *Bais et al.*, 1993; *Borowski et al.*, 1977; *Blumthaler and Ambach*, 1994; *Josefsson and Landelius*, 2000; *Grant and Heisler*, 2000; *Chubarova*, 1998; *Bodhaine et al.*, 1996]. The quality of the CMF parameterization depends largely on the quality and length of the measurement time series that are analyzed for the parameterization.

[6] Usually, no spectral dependence is considered, and the CMF parameterization is made for spectrally integrated UV global irradiance, such as UV-B and erythema-integrals. However, *Seckmeyer et al.* [1996b] showed that the CMF values are spectrally dependent. It is known that the ground albedo has influence on radiative cloud effects due to multiple reflections between the ground and the clouds and, as a consequence, on CMFs [*Kylling et al.*, 1997]. This aspect however is usually not taken into account in CMF parameterizations. The same is true for the dependence of CMFs on solar zenith angle. The study by *Josefsson and Landelius* [2000] suggests that this dependence is negligible. In an actual case, beside cloud amount and optical depth of the clouds, the exact position of the clouds in the sky plays an important role for the ground-level UV radiation. If a cloud obscures the solar disc, the irradiance is strongly reduced. On the other hand, for clouds with a position besides the Sun, enhancements of UV radiation at the ground compared to the cloud-free case by up to 20% or even more are observed [*Laird and Harshvardhan*, 1997; *Mims and Frederick*, 1994]. The CMF parameterizations, which result in averages, are unable to reproduce such individual cases. However, recent work [*Bodeker and McKenzie*, 1996; *Bordewijk et al.*, 1995; *Ito et al.*, 1993;

Grant and Heisler, 2000] suggests the use of a CMF parameterization that includes in the parameter record a broadband radiation measurement outside the UV spectral range; this measurement is often available with sufficient temporal resolution. The idea is that the broadband radiation measurement represents a snapshot of the interaction of the cloud field with the solar radiation and thus can be used to model the UV irradiance with higher precision even for actual cases.

[7] In this paper a comprehensive analysis of CMFs is presented, based on 2 years of continuous spectral UV measurements at one site in Germany. A new approach based on the neural network technique for the derivation of CMF parameterizations with five different types of cloud description is presented. Special attention is drawn to the question of how the quality of the CMF parameterizations changes for different parameter record qualities. Included is an evaluation of one of the CMF parameterizations using broadband radiation measurements for two other locations in Germany with different climatic conditions, in order to see whether the CMF parameterization is transferable. The dependencies of the average CMFs on relevant parameters, such as wavelength and solar zenith angle are investigated.

2. Method

2.1. General Aspects

[8] A 2-year time series of spectral UV global irradiance measurements carried out with a double monochromator at the Fraunhofer Institute for Atmospheric Environmental Research (IFU) in Garmisch Partenkirchen, Germany, was used to derive spectral CMF values. The corresponding clear-sky spectra are simulated with a rigorous radiative transfer model since clear-sky spectra are rare within the 2-year data record and are not available for all solar zenith angles and atmospheric conditions. To ensure that the agreement between measurements and modeling is the best, the instrument properties and the special conditions of the measuring site in Garmisch Partenkirchen are taken into account.

[9] The derivation of the CMF values is carried out with equation (1), where E_{cloud} is the measured spectral global irradiance in the presence of clouds and E_{clear} is the modeled spectral global irradiance for cloudless sky. Both quantities are spectrally dependent. Since spectral CMFs do not show any small-scale variations with respect to wavelength, the CMF analysis is made on the basis of only six wavelengths in the UV: 300, 305, 310, 321, 342, and 380 nm.

[10] To combine modeled with measured spectra, there are some requirements. First, the state of the atmosphere (ozone amount, aerosol conditions, albedo, etc.) for the conditions during the measurement has to be known to ensure that the simulated clear-sky spectrum corresponds to the measured spectrum. Second, the atmospheric conditions during the time of the measurement have to be stable. Since the measurement is a scanning procedure taking up to eight minutes, it is possible that cloud conditions change significantly within this time. If, for example, a cloud obscures the Sun during the scan, the measured spectrum is not homogeneous and the derivation of a spectral CMF value is no longer possible. To avoid this problem, every measured spectrum is checked for its stability.

Table 1. Data Within the Five Parameter Records

Parameter	Parameter Record				
	1	2	3	4	5
Solar zenith angle	X	X	X	X	X
Ground albedo	X	X	X	X	X
Total cloud amount	X	X	X	X	X
Cloud amount and cloud type for three different layers		X	X		
Flag whether solar disk is obscured or not			X		
Broadband solar irradiance				X	
Broadband visible irradiance (illuminance)					X

[11] For the derivation of different CMF parameterizations every CMF value is combined with different sets of parameters describing the corresponding sky situation (Table 1). As the parameterization tool the technique of neural networks [Landau and Taylor, 1998] is chosen. From the training of the neural networks, five different CMF parameterizations were obtained that allow the calculation of spectral CMFs from different parameter records. The resulting data are used for detailed studies of the different information content within the parameter records, i.e., the different sets of parameters of Table 1, and the dependence of average CMFs on solar zenith angle and wavelength.

2.2. Spectral UV Irradiance for Cloudy Conditions

[12] UV irradiance under cloudy conditions was taken from spectral measurements at the IFU site during the years 1996 and 1997, performed with a Bentham double monochromator. The measuring site is located at 47.49°N and 11.07°E at 730 m above sea level in a valley of the northern Alps. During daytime hours about 60 spectra per day are recorded. Because of the surrounding mountains only those spectra were used for the study when the Sun was at least 2° above the mountain ridge. Approximately 40,000 individual spectra for a wide range of cloud conditions could be used for further analysis. The solar zenith angle covers the range between 25° and 80°.

[13] As already mentioned, the derivation of CMF values requires additional data to describe the state of the atmosphere. At the IFU total ozone column and spectral aerosol optical depth are available throughout the day as long as the solar disk is not obscured by clouds [Mayer and Seckmeyer, 1998; Mayer et al., 1997]. These are obtained from spectral measurements of direct radiation in the UV wavelength range using a Sun tracker. Moreover, total solar irradiance measured by pyranometer and illuminance measured by luxmeter are available with high temporal resolution. Not provided are actual measurements of the vertical ozone profile and the absorption properties of the aerosols. More details about the measuring site, the instruments, the data analysis, the instrument stability checks and the calibration procedures are given by Seckmeyer and Bernhard [1993], Seckmeyer et al. [1994, 1996a], and Mayer et al. [1997]. For a well-maintained instrument, as used in this study, the absolute uncertainty is as high as 12.7% at 300 nm and 6.3% for erythemal weighted irradiance [Bernhard and Seckmeyer,

1999]. Major reasons are uncertainties in the calibration of the system and wavelength uncertainties.

[14] The other requirement is stable atmospheric conditions during the time of the UV scan, which lasts up to eight minutes. The stability check of every spectrum is carried out by analyzing a series of pyranometer measurements taken at 1-min intervals during the UV scan. As a stability criterion the standard deviation divided by the average is used with a threshold of 0.05. This demand leads to a huge reduction of the database. Applying this procedure for quality assurance to the spectral data leaves only about 10,000 from the total 40,000 spectra for further analysis.

2.3. Spectral UV Irradiance for Clear-Sky Conditions

[15] To every measured UV spectrum for cloudy conditions a corresponding clear-sky spectrum was modeled where all atmospheric conditions, except the clouds, represent the state of the atmosphere during the measurement. The radiative transfer model used is STARsci, a matrix operator model based on the discrete ordinate method [Ruggaber et al., 1994; Schwander et al., 2001, available <http://www.meteo.physik.uni-muenchen.de/strahlung/uvrad/Star/starprog.html>]. Its high quality is documented by model comparisons during recent years [Koepke et al., 1998; vanWeele et al., 2000; DeBacker et al., 2001]. The spectra for the IFU site were modeled using the provided spectral aerosol optical depth and the total ozone amount and simulating slit function and cosine response of the measuring instrument. Albedo values of 0.03 were assumed if no snow cover was present [Wang and Lenoble, 1994; Zeng et al., 1994]. For conditions with snow, the regional albedo was determined via snow height and snow age, applying the algorithm introduced by Schwander et al. [1999]. Since no information about the absorption properties of the tropospheric aerosols was available, assumptions about the aerosol absorption had to be made. The generally low optical depths throughout the year suggest the choice of a continental clean aerosol model [Hess et al., 1998] for the tropospheric aerosols, resulting in a single scattering albedo of about 0.96 in the UV.

[16] Special problems arise if the solar disk is not visible for the whole day, since ozone amount and aerosol optical depth data are therefore not available. In these cases, aerosol optical depth is interpolated between the last measurement before and the next measurement afterwards. Ozone values are taken from the measurements at Hohenpeissenberg, located at 47°25'N, 10°59'E, at a distance of about 30 km, adapted to the conditions in Garmisch Partenkirchen. For this adaptation a time series of total ozone amounts from Hohenpeissenberg and Garmisch Partenkirchen were homogenized, leading to a modification of the Hohenpeissenberg values by a factor of about 1.025 to represent the conditions at Garmisch Partenkirchen, that has higher ozone values due to the lower elevation above sea level. If no ozone value was available at Hohenpeissenberg either, the data of the corresponding day were omitted since a temporal interpolation of ozone values may lead to large deviations. The influence of the surrounding mountains that prevent an unrestricted view to the horizon was taken into account within the model. The high quality of the agreement within ±10% between modeled and measured values for

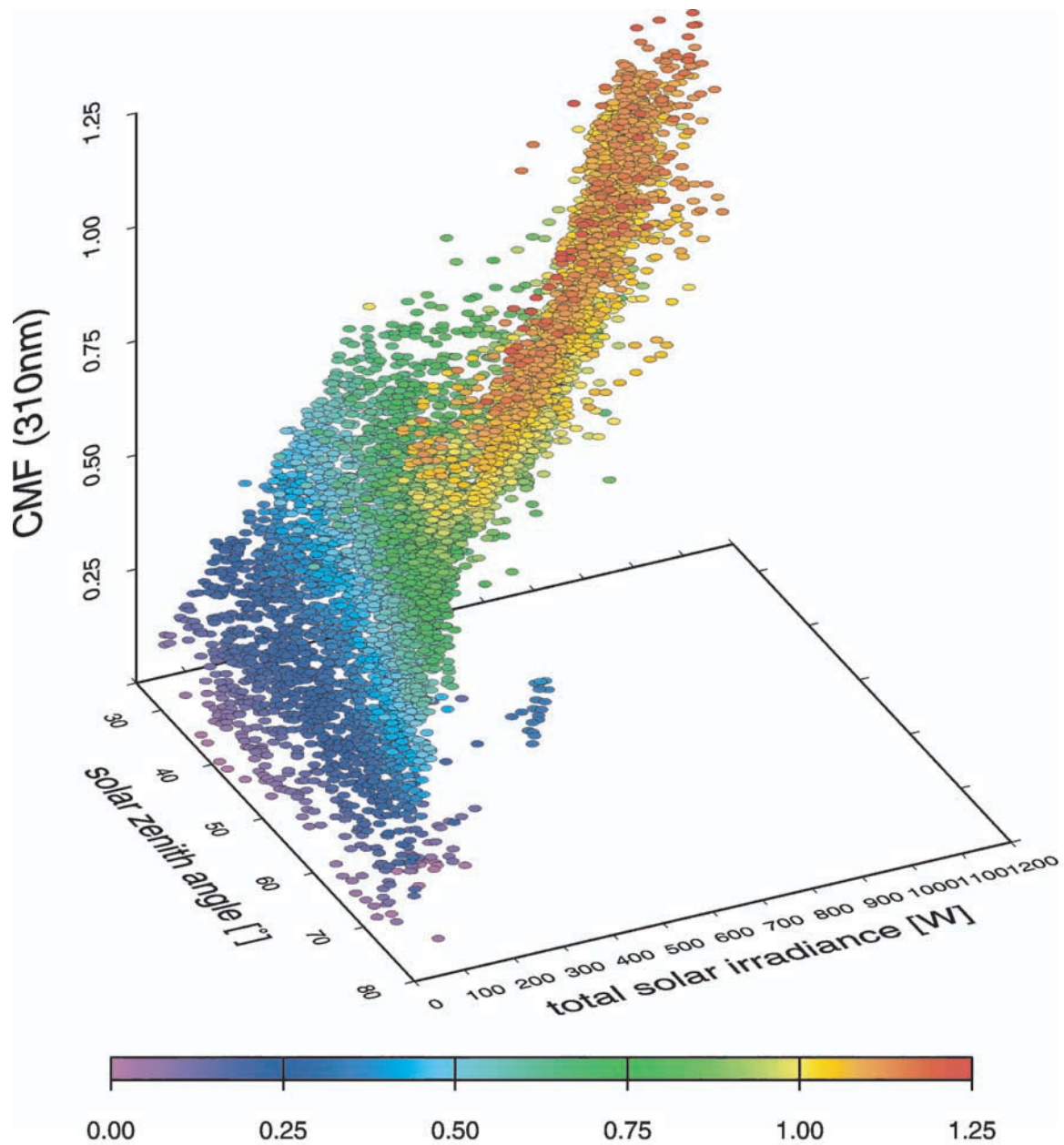


Figure 1. Relationship between CMF at 310 nm, total solar radiation, measured by a pyranometer, and solar zenith angle.

cloud-free conditions within the 2 years is shown by Schwander *et al.* [1999].

[17] From both measurements and modeling the CMF values at six wavelengths for 9000 remaining atmospheric conditions could be derived, comprising the database for the further analysis.

2.4. Variable Descriptions of the Cloud Conditions

[18] To describe the interaction of the clouds with the radiation field via CMF an adequate description of the sky conditions is necessary. This description may be composed of (1) data that describe the cloud conditions, (2) data that mirror important features of the radiation field, and/or (3) data that reproduce directly the interaction between clouds

and radiation field. For all three descriptions a compromise between availability of the data and information content has to be found.

1. The information that is generally available is cloud observations by the Meteorological Services. In Garmisch Partenkirchen such an observatory is operated by the German Meteorological Service (DWD). It is located at 47.50°N and 11.10°E, 720 m above sea level (asl), with a distance of about 1 km from the IFU UV measuring site. Cloud observations are available every hour on the hour. Therefore, one cloud observation is associated with all CMF values between 30 min before and 30 min after the full hour. The observations are converted into a cloud description giving the total cloud amount in okta and the cloud amount

and cloud type for low, medium-high, and high clouds. From measurements of the direct Sun at the IFU site, a distinction as to whether the solar disk is obscured by clouds or not can be drawn easily.

2. Even for a distinct cloud situation its effect on the radiation field may depend significantly on solar zenith angle and on atmospheric conditions in the troposphere. With solar zenith angle the ratio of direct to diffuse irradiance changes, and thus the CMF for a distinct cloud situation may change. Among the atmospheric conditions the surface albedo is of major importance for the CMF due to multiple reflections between the ground and clouds. Furthermore, the amount of variable tropospheric scattering and absorbing particles and gases (i.e., aerosols and ozone) is of relevance due to cloud-induced photon path length variations.

3. Broadband irradiance measurements such as total solar radiation and illuminance, or measurements with a filter radiometer, during the UV scan can be used to parameterize the interaction of the clouds with the radiation field. These measurements contain information about the total radiation level and, together with solar zenith angle, about the modification of radiation by clouds. The close relationship between CMF values, solar zenith angle, and broadband irradiance is demonstrated in Figure 1.

[19] From these three categories, five different sets of data, representing different quality and availability, are arranged to describe the sky conditions. The data sets (Table 1) are composed of solar zenith angle, ground albedo, total cloud amount, cloud amount and cloud type of low, medium-high and high clouds, information, whether the solar disk is obscured by clouds, total solar irradiance measured by Pyranometer (average during the UV scan), and illuminance measured by Luxmeter (average during the UV scan). In the following, for simplicity, the five data sets in Table 1 are indicated by parameter record 1 to 5.

[20] Parameters of category 1 are more or less detailed cloud descriptions, used in parameter records 1 to 3. Parameters of category 2 are solar zenith angle and ground albedo, used in all parameter records. Tropospheric ozone content and tropospheric aerosol properties were not included as parameters of category 2. The reason tropospheric ozone content was omitted is the lack of measurements. Total ozone is not appropriate since it represents mainly the stratospheric ozone content, which has only minor interactions with cloud effects. Aerosol optical depth was not chosen as a parameter of category 2, though aerosol optical depth is primarily determined by the tropospheric aerosol. The reason is that the decision cannot be made as to whether a measured high aerosol optical depth is caused by aerosols or by a thin cirrus cloud. Moreover, no information about the absorption properties of the tropospheric aerosols is available.

[21] Parameters of category 3 are the total solar irradiance and illuminance. They are used in parameter records 4 and 5. Even in these parameter records the total cloud amount is taken into account to supply some information on how the modification of the radiation field by clouds in the broadband is converted to the UV spectral range. For example, the radiation is more influenced by a single cloud that obscures

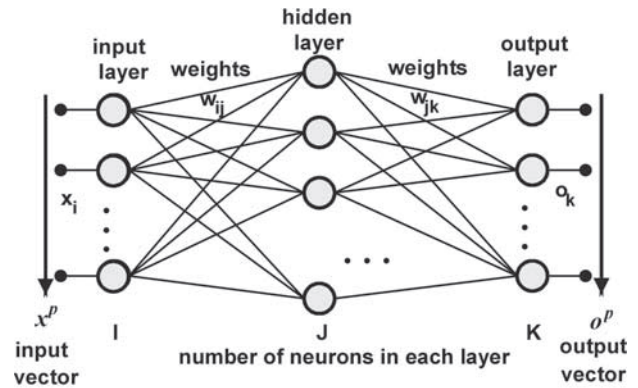


Figure 2. Schematic illustration of a feed forward perceptron-type neural network.

the solar disk in the visible than in the UV, since a larger portion of the radiation is diffuse in the UV.

2.5. Neural Networks

[22] To find a CMF parameterization, i.e., to analyze the relationship between the CMF values and the different parameter records mentioned in section 2.4, neural networks were chosen. They have some advantages compared to other analysis techniques, such as regression analysis. Neural networks are able to approximate a functional dependence describing the best relationship between the spectral CMF values (target) and the parameter record (input) by a training procedure, and no functional dependency has to be given a priori [Landau and Taylor, 1998]. This procedure is carried out by minimizing the root mean square error (RMSE) between the target values and the calculated CMFs of the neural network (output). Neural networks are able to approximate any nonlinear function between the input and target data during training. This is an advantage, especially for the CMF analysis, since their dependencies based on effects of multiple scattering are highly nonlinear. For the dependencies found by the training of the neural networks, there is no chance and no need to give a simple formula.

[23] A schematic illustration of a neural network used for this study is given in Figure 2. It consists of one layer of input neurons, one layer of output neurons, and one or more hidden layers in between. The number of neurons for the input layer is determined by the available information (in our case the size of the parameter record) and for the output layer by the target information (in our case the number of spectral CMF values). The choice of the number of hidden layers in between and their size depends on the task and is made on the basis of experience. The neural network shown in Figure 2 represents a perceptron-type feed-forward net, which means that the network is fully interconnected between the neurons of one layer to all neurons of the adjacent layers. Every connection represents a weight $w_{i,j}$, responsible for the modification of the signal propagating from neuron n_i to neuron n_j . At the neuron n_j all signals from the neurons n_i of the layer in front arrive, modified by the weights $w_{i,j}$. The signals are added up and passed through a sigmoid function, yielding a signal which is sent

out to the following neurons n_k . It has been proven that a neural network with one hidden layer is already able to reproduce any nonlinear functional dependence between the input and target data [Hornik and Stincombe, 1989]. By training of a neural network the weights $w_{i,j}$ are determined in such a way that the neural network is able to reproduce the functional dependence between input and target vectors.

[24] The weights $w_{i,j}$ are initialized randomly before the training of a neural network is carried out. Taking the first pair of input and corresponding target vector, the input data propagate through the neural network and the output data are compared to the target data. The calculated RMSE between output and target data back propagates through the network and is used by the training algorithm to adapt the weights. This is carried out for each pair of input and target vectors and is called one epoch of training. This scheme is done iteratively with randomized order of training data for each epoch. The training is finished if the averaged RMSE of one epoch no longer decreases significantly or a user-defined threshold for the RMSE is reached.

[25] In our case, five different neural network configurations were trained for five different input parameter records (Table 1). The number of input neurons is different for the five neural networks varying between three (parameter records 1, 4, 5) and 10 (parameter record 3). The number of output neurons is always six, corresponding to the six derived spectral CMF values. For each network two hidden layers with six neurons in each layer was chosen. By testing various training algorithms, back percolation [Jurik, 1990] showed the best results and was chosen to train all networks. The training of the neural networks was finished after 20,000 to 50,000 epochs, depending on the input data set used.

2.6. Evaluation of CMF Parameterization

[26] Generally, the portability of the functional dependence (CMF parameterization) between CMF and parameter record derived with data from one specific location to other locations depends on the kind of the underlying parameter record. Using a visual description of cloudiness (category 1 in section 2.4), the portability is restricted to places with a comparable cloud climatology. If, for example, at location B cumulus clouds feature significantly higher optical depths than for location A, used for CMF parameterization, the application of the CMF parameterization for A will not be appropriate to describe the modification of UV irradiance by cumulus clouds at B. Using an actually measured broadband radiation quantity within the parameter record (category 3 in section 2.4) for the parameterization of the CMF values these restrictions cease to exist since, in the mentioned example, the stronger radiative effects of the cumulus clouds due to their higher optical depths are implicitly taken into account in the radiation quantity. Hence, the focus for the evaluation of CMF parameterization by the neural network algorithms is placed on those using a parameter record including a radiation quantity.

[27] To test the portability of these CMF parameterizations, further spectral UV measurements under cloudy conditions, carried out within the UV monitoring network of the Bundesamt für Strahlenschutz (BfS) are used, with two measuring sites in different climates. One is Offenbach (50°0'17"N, 8°39'04"E, 110 m asl), a continental station in

the middle of Germany, and the other is Zingst (54°26'19"N, 12°43'25"E, 5 m asl) a maritime station near the Baltic sea. Measurements carried out with a Bentham Double monochromator are taken every six minutes during daylight. All spectra measured at the two stations in 1998, i.e., about 60,000, were used for the analysis. Actual ozone amounts, interpolated from nearby ground-based Dobson measurements, were used for the clear-sky modeling. Albedo values during snow cover were derived as at the IFU site [Schwander et al., 1999]. For conditions without snow the albedo was set to 3%. No information was available for the actual aerosol conditions. Hence, the aerosol properties (optical depth, single scattering albedo, etc.) were kept constant in the model throughout the year, but using different aerosol types [Hess et al., 1998]. For both stations an aerosol optical depth of 0.2 was chosen and the boundary layer aerosol was assumed to be average continental in Offenbach and maritime polluted in Zingst. All clear-sky spectra were modeled taking into account the true cosine response and the true slit function of the measuring instruments.

[28] Every measurement under cloudy conditions was compared with model results using the spectral CMF values derived from the CMF parameterization using parameter record 4. Parameter record 5 could not be tested, since the BfS measuring sites do not provide actual luxmeter measurements. The actual cloud amount and the pyranometer data, needed as input for the CMF algorithm, were available at every measuring site. Inhomogeneous measured UV spectra (varying atmospheric conditions during the time of the UV scan, especially due to variable cloud conditions) were not identified and therefore not eliminated from the data. Because of the huge amount of data the comparison is carried out not on the basis of spectral UV irradiances but on erythemally integrated UV irradiances.

3. Results

3.1. Quality of the CMF Parameterizations

[29] To illustrate the ability of the CMF parameterizations to produce adequate CMFs on the basis of different parameter records, the predicted CMFs are plotted in Figure 3 against the "true" CMF values, i.e., the CMF values from the ratio of the individual UV measurements and the corresponding clear-sky result, used for the training of the neural networks. Figure 3a shows the results for parameter record 1, Figure 3b for parameter record 2, 3c for 3, and 3d for 5. The data points in all figures represent the average CMF for the six CMF wavelengths. No figure is shown for parameter record 4 since the results look quite similar to those of parameter record 5. The lines in the figures indicate $\pm 10\%$ and $\pm 50\%$ agreement bands of the CMF values. As a consequence of equation (1), this agreement of the CMF values also describes the quality of the agreement between modeled and measured UV global irradiance under cloudy conditions.

[30] In CMF parameterization 1 the cloud influence is predicted from the solar zenith angle, the ground albedo and the total cloud amount (Figure 3a). This parameterization results in an accumulation of data points for CMFs around unity. These are cases of small cloud amounts. For predicted CMFs around unity, however, some CMF values in reality are below 0.5. These cases occur if even for small cloud amounts the cloud obscures the solar disk. The CMF

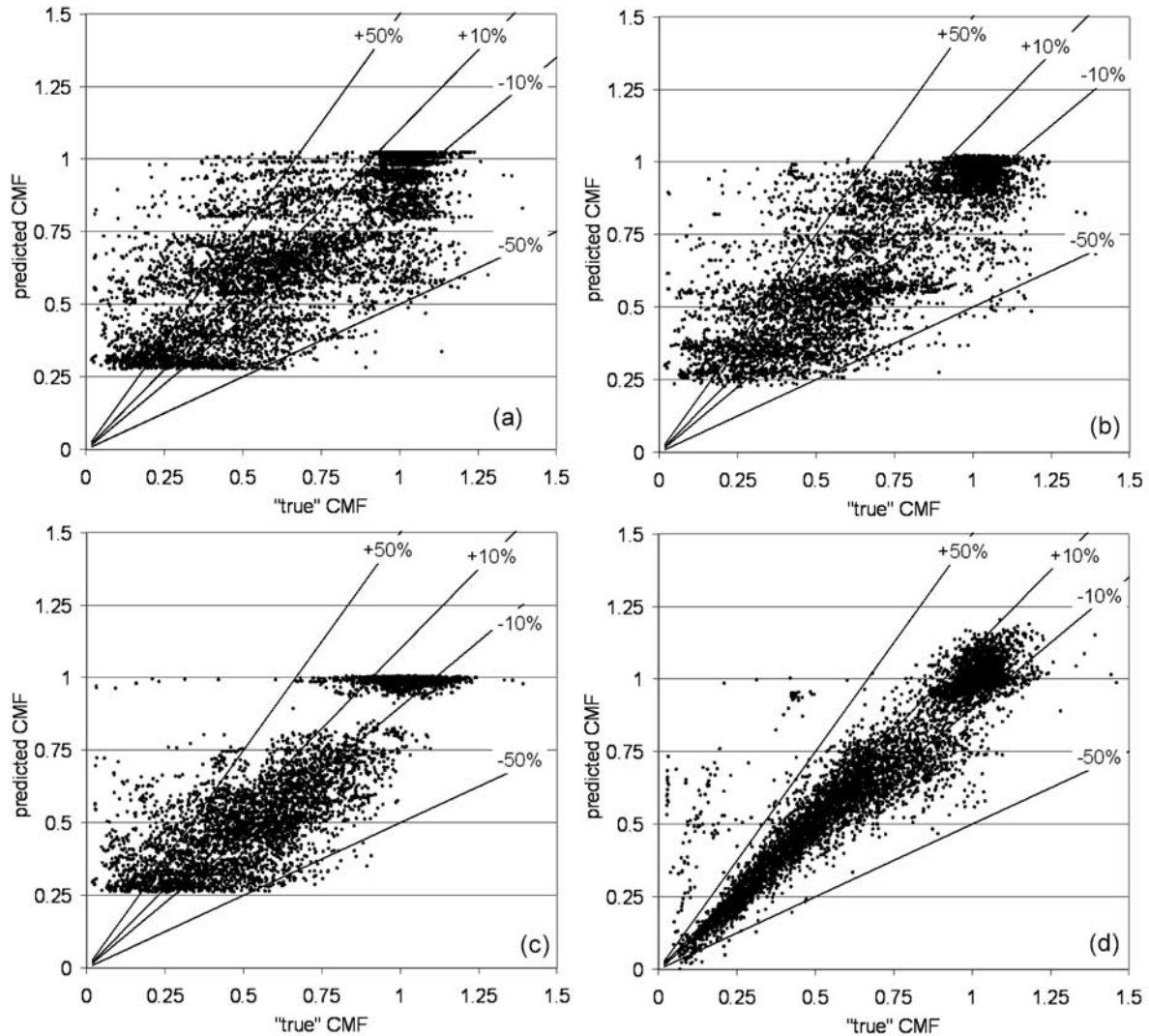


Figure 3. Scatterplot between true and predicted CMF (average CMF for six wavelengths mentioned in text) for (a) parameter record 1, (b) parameter record 2, (c) parameter record 3, and (d) parameter record 5. For details, see text.

parameterization cannot distinguish when this case occurs since the input data provide no information for this decision. Maximum CMFs produced by this CMF parameterization do not exceed unity, though the true CMF values range up to 1.25. This enhancement of UV irradiance due to conditions with broken cloudiness is caused if the solar disk is not obscured by clouds and diffuse radiation is enhanced, e.g., by reflection of radiation at nearby cloud edges [Mims and Frederick, 1994]. On the basis of the parameter record 1 used, the neural network is not able to reproduce these data, and averages such enhancements with other cases when the irradiance is not enhanced or even decreased. For higher cloud amounts the CMF parameterization gives CMFs as low as 0.25. This average value for overcast conditions results from the averaging between optically thin (cirrus) and optically thick (cumulus, stratus) clouds, since the only information about the cloud situation in the CMF parameterization 1 is the total cloud amount. The agreement with the true CMF values is rarely within $\pm 10\%$ and there are many

data points outside the $\pm 50\%$ agreement range. The average absolute error (taken to avoid the averaging of positive and negative deviations) of all cases is 0.141 in the UVB and 0.135 in the UVA wavelength range. A complete list of these errors for all CMF parameterizations is given in Table 2.

[31] CMF parameterization 2 includes a separation between optically thin and thick clouds since the input data comprise cloud amount and cloud type for low, medium-

Table 2. Average Absolute CMF Error Using CMF Parameterizations 1 to 5

CMF Parameterization	Wavelength Range	
	UVB	UVA
1	0.141	0.135
2	0.121	0.110
3	0.102	0.093
4	0.073	0.062
5	0.073	0.076

high and high clouds, beside total cloud amount (Figure 3b). Compared to Figure 3a, the number of predicted CMFs close to unity has increased. High cirrus clouds decrease UV irradiance only marginally and the CMF parameterization is now able to separate these cloud situations from others. The scattering of the data points in the horizontal direction is a bit smaller compared to Figure 3a. This is a consequence of the separation between medium-high and low clouds and different cloud types, since their typical optical depths differ considerably [Hughes, 1984; Hess *et al.*, 1998]. The average absolute error for this CMF parameterization 2 drops, compared to parameterization 1, to 0.121 in the UVB and to 0.110 in the UVA (Table 2). The still large scattering of the points is caused, on the one hand, by the remaining strong variability of optical depths within the cloud types and, on the other hand, by the unknown position of the clouds relative to the Sun.

[32] The latter is changed with CMF parameterization 3 (Figure 3c), where the information as to whether or not the solar disk is obscured by clouds is taken into account. Compared to Figure 3a and 3b, the scatter in the figure is significantly reduced. The average absolute error decreases to 0.102 in the UVB and 0.093 in the UVA (Table 2). However, especially for low CMFs, deviations of more than 50% still occur. The main reason is the unknown optical depth of the clouds in an actual case. The classification of the cloud situation with cloud amount, cloud level and cloud type is inadequate to reproduce the cloud optical depths with better accuracy. Besides the scattering in Figure 3c for low CMFs, there is a clear accumulation of predicted CMFs around unity whereas the true CMF values spread from 0.75 to 1.25. Besides high cirrus clouds these results are produced by conditions with broken cloudiness when the solar disk is visible. These situations may lead to a range of CMF values significantly above unity, but also to values below 0.8 depending on the position of the clouds relative to the observer. The information that the solar disk is not obscured is not sufficient to conclude if the clouds enhance or decrease UV irradiance. The CMF description averages these cases and produces CMFs around unity. Consequently, there is a gap between predicted CMFs close to unity and below 0.8.

[33] Figure 3d shows the results of the CMF parameterization 5, where a broadband irradiance measurement, here the illuminance measured by a luxmeter, is part of the parameter record. The agreement between predicted CMFs and true CMF values is now dominating within $\pm 15\%$. The average absolute error for the CMF parameterizations 5 (and also for parameterization 4) is now around 0.06 for both wavelength regions (Table 2). Even now some data points, less than 1%, are significantly outside this agreement range, on the left side of the scatterplot. They have been identified as representing two specific continuous time periods of several days with high irradiances both for luxmeter and pyranometer but very low values for the UV radiometer. Both periods started with huge amount of fresh snow, which probably influenced the optics of the UV radiometer.

[34] Because of the radiation measurements used as input data, the CMF parameterization is now able to produce CMFs lower than 0.25 and higher than unity. The application of the broadband measurement gives information about the interaction of the clouds with the radiation field, and the

CMF parameterization is able to transfer this information to the UV wavelength range. Using such broadband information, a radiative transfer model combined with CMF parameterization 4 or 5 allows the reproduction of the UV global irradiance measurements in Garmisch Partenkirchen with deviations around $\pm 15\%$ for all cloud conditions.

3.2. Evaluation of the CMF Parameterization

[35] About 60,000 spectra modeled for cloudy conditions using the CMF parameterization 4 were compared with measured spectra of two stations in Germany with different climatic conditions, mentioned in section 2.6. As an example, Figure 4 shows the comparison for Offenbach for erythemally weighted integrals, split into categories of different cloudiness. Figure 4a gives the scatterplot for cloud amount up to 3 oktas, Figure 4b for 3–6 oktas and Figure 4c for 7 and 8 oktas. The lines in the figure represent an agreement within $\pm 15\%$. For cloud amount less than 3 oktas the general agreement is mostly within the two lines. Keeping in mind that no actual aerosol information was available, and that the aerosol properties were kept constant, deviations on the order of $\pm 15\%$ have to be expected [Schwander *et al.*, 1997]. For higher cloud amount (Figures 4b and 4c) the deviations remain within this range confirming the quality of the CMF parameterization. Only for signals less than 0.05 W/m^2 does the agreement between model and measurement become slightly worse. These are signals that result in an UV index (UVI) [World Meteorological Organization (WMO), 1997] less than two and are thus of low risk for human erythema. Though the CMF parameterization is applied to data with other climatic conditions, the quality of the results is not worse than for the Garmisch Partenkirchen data derived for continental alpine conditions.

[36] Another quality test of measured and modeled data is the comparison of UV-index values for 1 year of measured data at Zingst for maritime climate conditions. The measured and modeled maximum daily UVIs (which are proposed to be used for public warning with respect to UV radiation [WMO, 1997]) are shown in Figure 5 together with their differences. Highest absolute differences occur for high UVI values, i.e., in summer. There is a slight tendency for higher measurements than modeling results during summer. This behavior is not only apparent for cloudy cases but for cloudless cases as well. Thus the reasons have to be found in measuring and modeling aspects outside the CMFs, which are investigated here.

[37] Figures 4 and 5 show that the CMF parameterization 4, using a broadband measurement as part of the information about the cloud conditions, can be applied to different sites with different climatological conditions in central Europe, even though it is derived on the basis of data for an alpine station.

3.3. Sensitivity Studies

[38] Sensitivity studies were carried out with the CMF parameterizations 1, 2, and 3, since they describe average conditions and thus allow the detection of features that may be masked in individual CMF values. Of major interest were the dependencies of the CMFs on wavelength and solar zenith angle for specific cloud situations. Remember, however, that the CMF parameterizations are the result of the training of neural networks. So the statistics of the

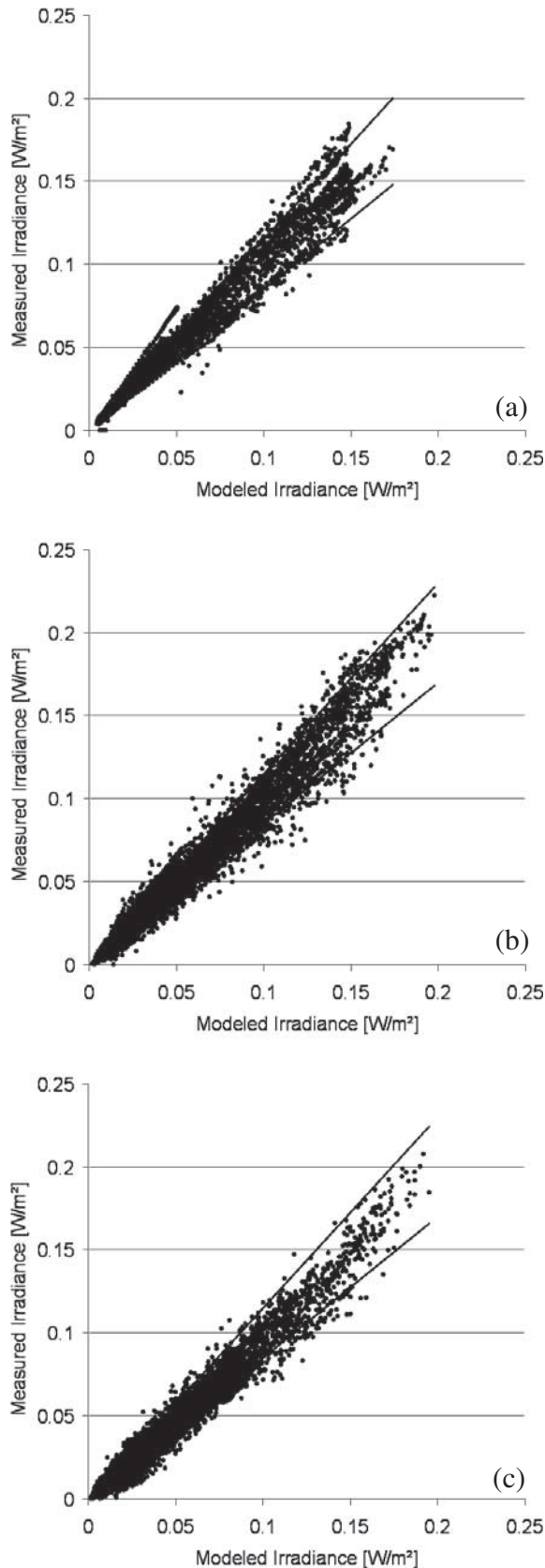


Figure 4. Scatterplot of modeled and measured irradiance (erythemal) at Offenbach for (a) cloud amount 0–2 oktas, (b) cloud amount 3–6 oktas, and (c) cloud amount 7–8 oktas using CMF parameterization 4 in the model.

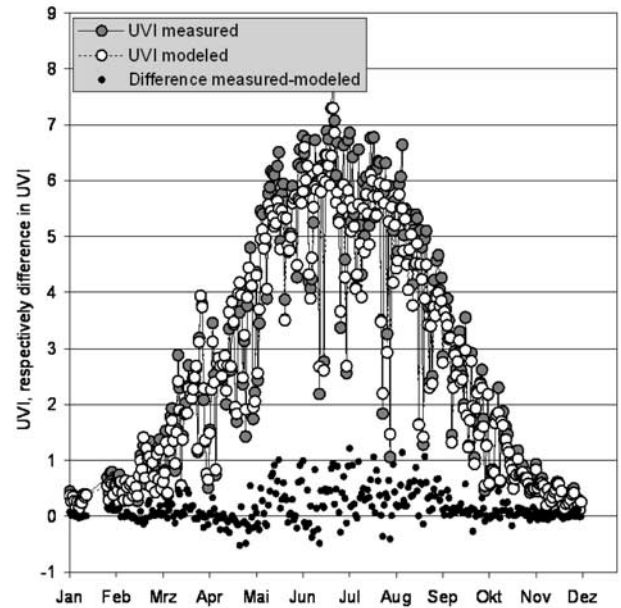


Figure 5. Daily UVI, calculated from spectral measurements and from model calculations using CMF parameterization 4 and their difference for Zings, Baltic Sea.

training data sets are also of major importance, especially for the sensitivity studies, which combine in the analysis data from different conditions. If, for example, a specific class of cloud amount is over represented by clouds with significantly different optical depth than other classes, the neural network will learn this feature. This may result in sensitivities not caused by the physics of the cloud interactions with the radiation field but rather biased by the statistics of the training data set. Therefore, it is important to focus the interpretation of the results on features that can be understood physically and ignore features that probably are based on bad statistics.

3.3.1. Dependency of the CMFs on wavelength

[39] As an example, Figure 6a shows the wavelength dependence for low clouds for cloud amounts from 1 to 8 oktas, represented by the symbol size. For overcast conditions (largest symbols) the CMFs increase (i.e., decrease of the cloud influence) with decreasing wavelength and, below a maximum around 315 nm, decrease again (increase of the cloud influence). Approaches with one-dimensional radiative transfer models and results derived from spectral measurements [Seckmeyer *et al.*, 1996b] show similar behavior of the wavelength dependence of the spectral CMF values. The increase of CMFs for overcast conditions with decreasing wavelength in the UVA is caused by photons, scattered back to the upper atmosphere by clouds and then scattered downward again [Kylling *et al.*, 1997]. Because of increasing optical depth of air molecules with decreasing wavelength these photons have a higher chance to be scattered downward again. Below about 310 nm this effect is overcompensated by increasing absorption of tropospheric ozone due to the increase of photon path length in the presence of clouds. For 8 oktas the CMF varies in the analyzed spectral range between 0.28 and 0.20, i.e. on the order of 40%. With decreasing cloud amount, Figure 6a

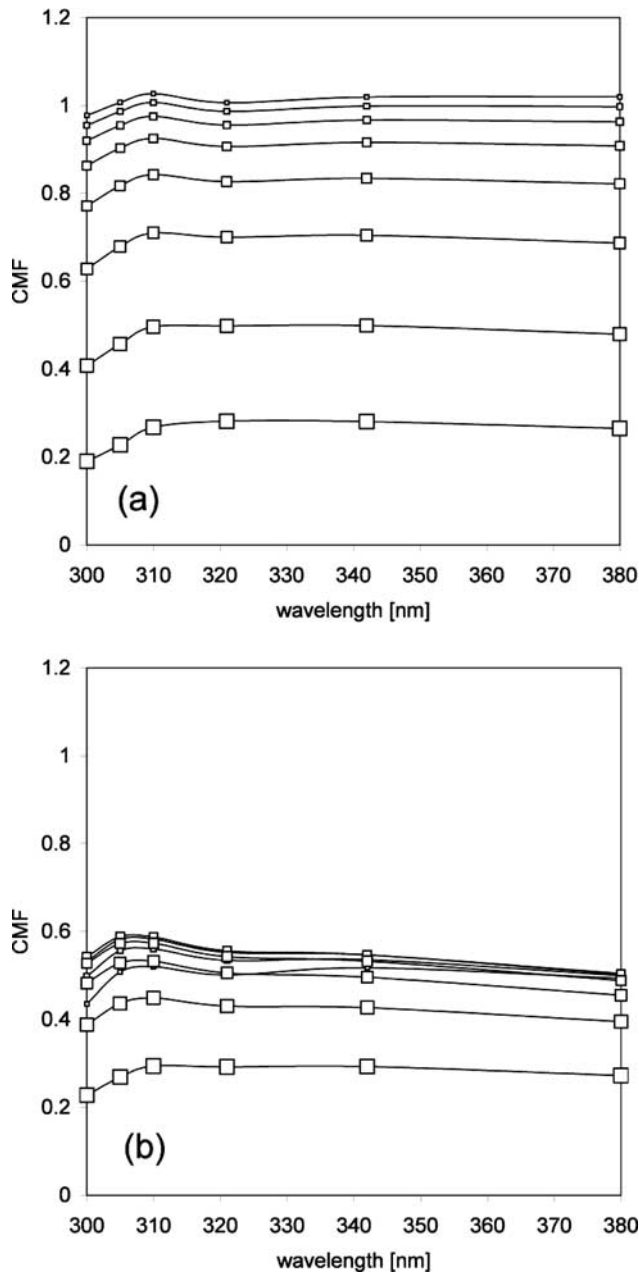


Figure 6. Spectral CMFs as function of cloud amount (large symbols, 8 oktas, down to 1 okta, smallest symbols) (a) using CMF parameterization 2 and (b) using CMF parameterization 3 with solar disk obscured by clouds.

shows in general a diminishing wavelength dependence of the CMF values. For 1 okta the spectral CMF variation is around 10%. The reason is that the smaller the areas with clouds are the smaller is the portion of photons scattered upward by the cloud tops and the smaller is the photon path length increase, which is responsible for the wavelength dependence.

[40] The same investigation is carried out for low clouds with the restriction to those cases when the solar disk is obscured by clouds. The results, shown in Figure 6b, are based on CMF parameterization 3. For overcast conditions the wavelength dependence does not change significantly

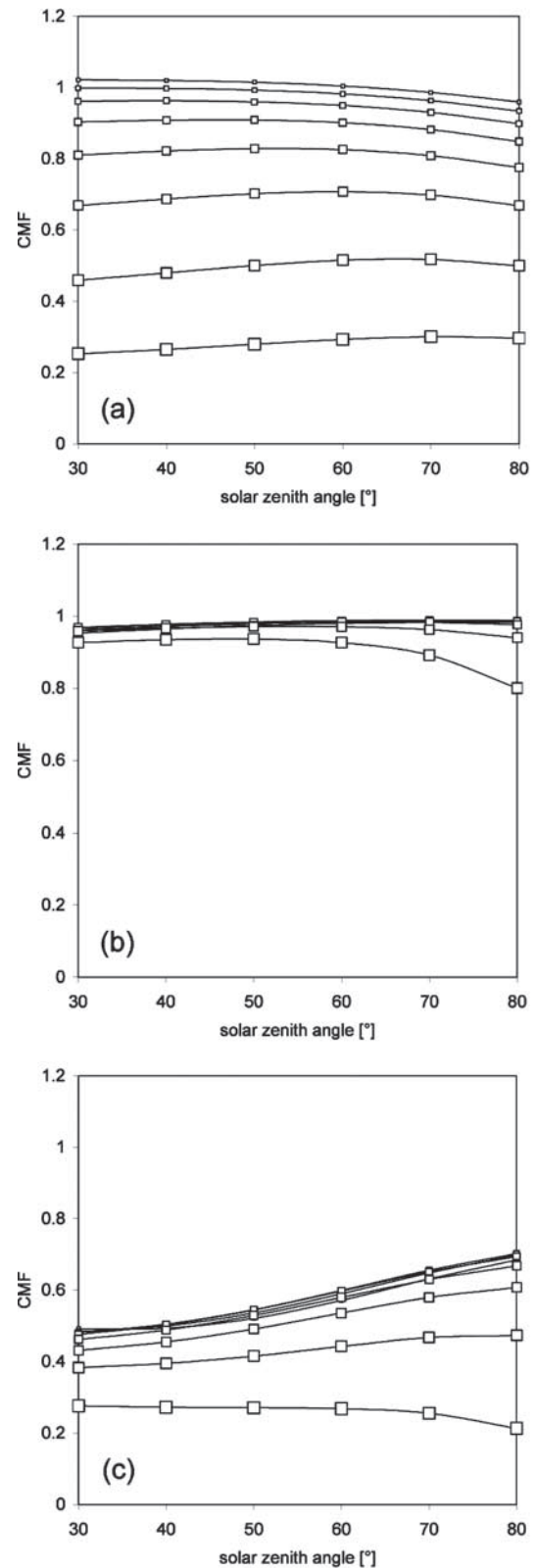


Figure 7. Dependence of CMF on solar zenith angle as function of cloud amount (large symbols: 8 oktas, down to 1 okta, smallest symbols, except Figure 7b, where 8 oktas are omitted and the largest symbol represents 7 oktas) (a) using CMF parameterization 2, (b) using CMF parameterization 3 with solar disk not obscured by clouds, and (c) using CMF parameterization 3 with solar disk obscured by clouds.

relative to that from Figure 6a since both lines describe the same conditions. The spectral dependence of the CMFs in Figure 6b seems to be more pronounced for low cloud amounts, with values in the order of 20%, contrary to Figure 6a. In general, for decreasing wavelength the contribution of direct irradiance to total irradiance decreases. If cloud amount is low, and a cloud obscures the solar disk, the effect on diffuse irradiance is negligible so that the CMF decreases significantly with shorter wavelength. With increasing cloud amount the diffuse irradiance is more and more affected in the same way as the direct irradiance, and the spectral dependence of the CMF is reduced.

3.3.2. Dependency of the CMFs on solar zenith angle

[41] The sensitivity of CMF on solar zenith angle is presented in Figure 7 for a wavelength of 380 nm and low clouds. Symbol size is again associated with cloud amount. No clear dependence of CMF on solar zenith angle can be seen in Figure 7a, valid for CMF parameterization 2. The sensitivity based on CMF parameterization 3 distinguishes between those cases when the Sun is visible (Figure 7b) and those cases when the solar disk is obscured by clouds (Figure 7c). If the Sun is visible (Figure 7b), again no clear impact of clouds on UV irradiance up to cloud amounts of 6 oktas can be seen. For a cloud amount of 7 oktas, however, the CMF decreases with increasing solar zenith angle. This behavior can be explained by the contribution of direct to total irradiance, which decreases strongly with increasing solar zenith angle. If a larger portion of the radiation is direct, high cloud amount has a weaker effect since the direct photons pass the cloud layers unperturbed.

[42] The opposite is true if the solar disk is obscured (Figure 7c). If cloud amount is low, the decrease of UV irradiance is weakest for high solar zenith angles, since the direct portion is low. With increasing cloud amount the differences for different solar zenith angles become smaller since the clouds interact more and more with the diffuse radiation in the same way as with direct radiation.

4. Conclusion

[43] A detailed analysis of spectral CMF values, derived from a combination of 2 years of spectral measurements and clear-sky model results, was carried out by using the analysis tool of neural networks. The results were investigated with emphasis on the different parameter records used to determine CMFs.

[44] These different parameter records produce different sensitivities of CMFs with respect to solar zenith angle and wavelength. A separation of CMFs between those cases when the solar disk is obscured by clouds or not results in significant dependencies of CMFs on solar zenith angle, while these effects vanish if this separation is not carried out. The known spectral dependence of the CMFs for overcast conditions is also modified in a different manner for different parameter records. As a consequence, general statements about the sensitivity of CMFs on other parameters should be drawn carefully.

[45] Parameter records compiled from ground-based visual cloud observations are generally inadequate to determine actual CMF values. With the information as to whether the solar disk is free or obscured by clouds in the

CMF parameterization, the results can be improved considerably. However, deviations of more than 50% occur frequently, and it is impossible to determine whether or not the UV irradiance is enhanced by clouds in an actual case. The remaining deviations result from the inadequate specification of both the cloud optical depth and position of the clouds by the introduced visual cloud description. Consequently, the integration of broadband measurements within the CMF parameterization improves the determination of CMFs for actual conditions significantly, to better than 15% in most of the cases. Moreover, this type of CMF parameterization is applicable for cloud conditions of different climates. In combination with a radiative transfer model such a CMF parameterization is able to calculate UV integrals with a quality not significantly worse compared with that of the clear-sky case. The employment of such an algorithm allows the conversion of pyranometer measurement sites to UV monitoring sites if at least the actual ozone amounts needed to run a clear-sky radiative transfer model are known.

[46] The algorithms and coefficients of the neural network are available on request as FORTRAN source code. They can be combined with any spectral radiative transfer model, though multiple scattering codes are strongly recommended. Especially the CMF parameterization 4 could be of special interest for the forecasting of UVI, if the total global irradiance is one of the forecasted parameters of a climate model.

[47] **Acknowledgments.** We would like to thank M. Steinmetz from the Bundesamt für Strahlenschutz, BfS and the German Meteorological Service, DWD, for providing their data. The study was funded by the German Ministry for Science and Technology, BMBF.

References

- Bais, A. F., C. S. Zerefos, C. Meleti, I. C. Ziomas, and K. Tourpali, Spectral measurement of solar UV-B radiation and its relations to total ozone, SO₂, and clouds, *J. Geophys. Res.*, 98(D3), 5199–5204, 1993.
- Bernhard, G., and G. Seckmeyer, Uncertainty of measurements of spectral UV irradiance, *J. Geophys. Res.*, 104(D12), 14,321–14,345, 1999.
- Blumthaler, M., and W. Ambach, Effects of cloudiness on global and diffuse irradiance in a high-mountain area, *Theor. Appl. Climatol.*, 50, 23–30, 1994.
- Bodeker, G. E., and R. L. McKenzie, An algorithm for inferring surface UV irradiance including cloud effects, *J. Appl. Meteorol.*, 35, 1860–1877, 1996.
- Bodhaine, B. A., R. L. McKenzie, P. V. Johnston, D. J. Hofmann, E. G. Dutton, R. C. Schnell, J. E. Barnes, S. C. Ryan, and M. Kotkamp, New ultraviolet spectroradiometer measurements at Mauna Loa Observatory, *Geophys. Res. Lett.*, 23(16), 2121–2124, 1996.
- Bordewijk, J. A., H. Slaper, H. A. J. M. Reinen, and E. Schlamann, Total solar radiation and the influence of clouds and aerosols on the biologically effective UV, *Geophys. Res. Lett.*, 22(16), 2151–2154, 1995.
- Borowski, J., A.-T. Chai, T. Mo, and A. E. O. Green, Cloud effects on middle ultraviolet global radiation, *Acta Geophys. Pol.*, 25(4), 287–301, 1977.
- Burrows, W. R., CART regression models for predicting UV radiation at the ground in the presence of cloud and other environment factors, *J. Appl. Meteorol.*, 36, 531–544, 1997.
- Cascinelli, N., and R. Marchesini, Increasing incidence of cutaneous melanoma, ultraviolet radiation and the clinician, *Photochem. Photobiol.*, 50(4), 497–505, 1989.
- Chubarova, N. E., Ultraviolet radiation under broken cloud conditions as inferred from many-year ground-based observations, *Atmos. Ocean*, 14(1), 131–135, 1998.
- DeBacker, H., et al., Comparison of measured and modelled UV indices, *Meteorol. Appl.*, 8, 267–277, 2001.
- Forster, P. M. D. F., Modeling ultraviolet radiation at the Earth's surface, part I. The sensitivity of ultraviolet irradiances to atmospheric changes, *J. Appl. Meteorol.*, 34, 2412–2425, 1995.

- Gleason, J. F., P. K. Bhartia, and J. R. Herman, Record low global ozone in 1992, *Science*, 260, 523–526, 1993.
- Grant, R. H., and G. M. Heisler, Estimation of ultraviolet-B irradiance under variable cloud conditions, *J. Appl. Meteorol.*, 39, 904–916, 2000.
- Hess, M., P. Koepke, and I. Schult, Optical properties of aerosols and clouds: The software package OPAC, *Bull. Am. Meteorol. Soc.*, 79(5), 831–844, 1998.
- Hornik, K. M., and R. W. Stincombe, Multilayer feedforward networks are universal approximators, *Neural Networks*, 2, 359–366, 1989.
- Hughes, N. A., Global cloud climatologies: A historical review, *J. Clim. Appl. Meteorol.*, 23, 724–751, 1984.
- Ito, T., Y. Sakoda, T. Uekubo, H. Naganuma, M. Fukuda, and M. Hayashi, Scientific application of UV-B observations from JMA network, paper presented at 13th UOEH International Symposium and the Second Pan Pacific Cooperative Symposium on Impact and Increased UV-B Exposure on Human Health and Ecosystems, Univ. of Occupational and Environ. Health, Kitakyushu, Japan, 1993.
- Josefsson, W., and T. Landelius, Effect of clouds on UV irradiance: As estimated from cloud amount, cloud tape, precipitation, global radiation, and sunshine duration, *J. Geophys. Res.*, 105(D4), 4927–4935, 2000.
- Jurik, M., Backpercolation: Exploiting the duality between signals and weights, report, Jurik Res., Aptos, Calif., 1990.
- Koepke, P., et al., Comparison of models used for UV index calculations, *Photochem. Photobiol.*, 67(6), 657–662, 1998.
- Koh, H. K., B. E. Kligler, and R. A. Lew, Sunlight and cutaneous malignant melanoma: Evidence for and against causation, *Photochem. Photobiol.*, 51(6), 765–779, 1990.
- Kylling, A., A. Albold, and G. Seckmeyer, Transmittance of a cloud is wavelength-dependent in the UV-range: Physical interpretation., *Geophys. Res. Lett.*, 24(4), 397–400, 1997.
- Laird, J. L., and Harshvardhan, Analysis of cumulus solar irradiance reflectance (CSIR) events, *Atmos. Res.*, 44, 317–332, 1997.
- Landau, L. J., and J. G. Taylor, *Concepts for Neural Networks: A Survey*, Springer-Verlag, New York, 1998.
- Mayer, B., and G. Seckmeyer, Retrieving ozone columns from spectral direct and global UV irradiance measurements, in *Proceedings of the XVIII Ozone Symposium, L'Aquila, Italy*, edited by R. D. Bojkov and G. Visconti, pp. 935–938, Edigrafital S.p.A.-S. Atto, Teramo, Italy, 1998.
- Mayer, B., G. Seckmeyer, and A. Kylling, Systematic long-term comparison of spectral UV measurements and UVSPEC modeling results, *J. Geophys. Res.*, 102(D7), 8755–8767, 1997.
- Mims, F. M., and J. E. Frederick, Cumulus clouds and UV-B, *Nature*, 371, 291, 1994.
- Ruggaber, A., R. Dlugi, and T. Nakajima, Modelling radiation quantities and photolysis frequencies in the troposphere, *J. Atmos. Chem.*, 18, 171–210, 1994.
- Schwander, H., P. Koepke, and A. Ruggaber, Uncertainties in modeled UV-irradiance due to limited accuracy and availability of input data, *J. Geophys. Res.*, 102(D8), 9419–9429, 1997.
- Schwander, H., B. Mayer, A. Ruggaber, A. Albold, G. Seckmeyer, and P. Koepke, Method to determine snow albedo values in the UV for radiative transfer modelling, *Appl. Opt.*, 38(18), 3869–3875, 1999.
- Schwander, H., A. Kaifel, A. Ruggaber, and P. Koepke, Spectral radiative-transfer modeling with minimized computation time by use of a neural-network technique, *Appl. Opt.*, 40(3), 331–335, 2001.
- Seckmeyer, G., and G. Bernhard, Cosine error correction of spectral UV-irradiance, *Atmos. Radiat.*, 2049, 140–151, 1993.
- Seckmeyer, G., et al., Intercomparison of spectral-UV-radiation measurement systems, *Appl. Opt.*, 33(33), 7805–7812, 1994.
- Seckmeyer, G., et al., Geographical differences in the UV measured by intercompared spectroradiometers, *Geophys. Res. Lett.*, 22(14), 1889–1892, 1995.
- Seckmeyer, G., G. Bernhard, B. Mayer, and R. Erb, High-accuracy spectroradiometry of solar ultraviolet radiation, *Meteorologia*, 32, 697–700, 1996a.
- Seckmeyer, G., R. Erb, and A. Albold, Transmittance of a cloud is wavelength-dependent in the UV-range, *Geophys. Res. Lett.*, 23(20), 2753–2755, 1996b.
- Stolarski, R. S., P. Bloomfield, R. D. M. Peters, and J. R. Herman, Total ozone trends deduced from Nimbus 7 TOMS data., *Geophys. Res. Lett.*, 18, 1015–1018, 1991.
- vanWeele, M., et al., From model intercomparison toward benchmark UV spectra for six real atmospheric cases, *J. Geophys. Res.*, 105(D4), 4915–4925, 2000.
- Wang, P., and J. Lenoble, Comparison between measurements and modelling of UV-B irradiance for clear sky: A case study, *Appl. Opt.*, 33(18), 3964–3971, 1994.
- Weih, P., and A. R. Webb, Accuracy of spectral UV model calculations, 1, Consideration of uncertainties in input parameters, *J. Geophys. Res.*, 102(D1), 1541–1550, 1997.
- World Meteorological Organization (WMO), Report of the WMO-WHO meeting of experts on standardization of UV indices and their dissemination to the public, Geneva, Switzerland, 1997.
- Zeng, J., R. McKenzie, K. Stammes, M. Wineland, and J. Rosen, Measured UV spectra compared with discrete ordinate method simulations, *J. Geophys. Res.*, 99(D11), 23,019–23,030, 1994.

A. Kaifel, Zentrum für Sonnenenergie- und Wasserstoff-Forschung, Hessbrühlstrasse 21c, D-70565 Stuttgart, Germany.

P. Koepke and H. Schwander, Meteorologisches Institut, Universität München, Theresienstrasse 37, D-80333 Munich, Germany. (peter.koepke@lrz.uni-muenchen.de)

G. Seckmeyer, Institut für Meteorologie und Klimatologie, Herrenhäuser Strasse 2, D-30419, Hannover Germany.